

GEOTECHNICAL SPECIAL PUBLICATION NO. 250

ADVANCES IN TRANSPORTATION GEOTECHNICS AND MATERIALS FOR SUSTAINABLE INFRASTRUCTURE

SELECTED PAPERS FROM THE PROCEEDINGS OF THE
GEO-HUBEI 2014 INTERNATIONAL CONFERENCE ON
SUSTAINABLE INFRASTRUCTURE

July 20-22, 2014
Yichang, Hubei, China

SPONSORED BY
The Geo-Institute of the American Society of Civil Engineers

EDITED BY
Rifat Bulut, Ph.D.
Sung-Chi Hsu, Ph.D.



Published by the American Society of Civil Engineers

This is a preview. [Click here to purchase the full publication.](#)

Published by American Society of Civil Engineers
1801 Alexander Bell Drive
Reston, Virginia, 20191-4382
www.asce.org/bookstore | ascelibrary.org

Any statements expressed in these materials are those of the individual authors and do not necessarily represent the views of ASCE, which takes no responsibility for any statement made herein. No reference made in this publication to any specific method, product, process, or service constitutes or implies an endorsement, recommendation, or warranty thereof by ASCE. The materials are for general information only and do not represent a standard of ASCE, nor are they intended as a reference in purchase specifications, contracts, regulations, statutes, or any other legal document. ASCE makes no representation or warranty of any kind, whether express or implied, concerning the accuracy, completeness, suitability, or utility of any information, apparatus, product, or process discussed in this publication, and assumes no liability therefor. The information contained in these materials should not be used without first securing competent advice with respect to its suitability for any general or specific application. Anyone utilizing such information assumes all liability arising from such use, including but not limited to infringement of any patent or patents.

ASCE and American Society of Civil Engineers—Registered in U.S. Patent and Trademark Office.

Photocopies and permissions. Permission to photocopy or reproduce material from ASCE publications can be requested by sending an e-mail to permissions@asce.org or by locating a title in ASCE's Civil Engineering Database (<http://cedb.asce.org>) or ASCE Library (<http://ascelibrary.org>) and using the “Permissions” link.

Errata: Errata, if any, can be found at <http://dx.doi.org/10.1061/9780784478509>

Copyright © 2014 by the American Society of Civil Engineers.
All Rights Reserved.
ISBN 978-0-7844-1359-3 (CD)
ISBN 978-0-7844-7850-9 (E-book PDF)
Manufactured in the United States of America.

This is a preview. [Click here to purchase the full publication.](#)

Preface

This Geotechnical Special Publication (GSP) contains 18 papers addressing a variety of current issues in the Unsaturated Soil, Seepage, and Environmental Geotechnics; Soil Behavior and Laboratory Testing. The technical programs for the GeoHubei International Conference struck a balance between the fundamental theories and field applications. These papers were presented at the GeoHubei International Conference held July 20-22, 2014, in Hubei, China. This GSP includes investigations and solutions from numerous countries. It expands ranges of tools that are available to engineers and scientists.

The following individuals have assisted in reviewing the papers: Marshall Addison, An Deng, Ceci Harman, G.T. Hong, Jeffrey Lee, Julie Q. Shang, Xianming Shi, Zhiming Si, Lubinda Walubita, Jingan Wang, Danny Xiao, Joey Yang, and Xiaoming Yang.

Table of Contents

Discrete Element Method Simulation of Granular Column Collapse	1
Elnaz Kermani, Tianbin Li, and Tong Qiu	
Evaluating Proposed Solutions for Equivalent Plane Strain Modeling of PVD Assisted Preloading	9
Ali Parsa-Pajouh, Behzad Fatahi, Hadi Khabbaz, and Philippe Vincent	
Equilibrium Matric Suctions in Subgrade Soils in Oklahoma Based on Thornthwaite Moisture Index (TMI)	17
Er Yue and Rifat Bulut	
Soil-Water Characteristics of Undisturbed Net-Like Red Soils in Xuancheng, China	25
Mingwu Wang, Peng Xu, Jian Li, and Shuai Qin	
Computation Module of Expansive Soil Crack Depth Considering Dry-Wet Cycles	33
Beixiao Shi, Shengshui Chen, and Guoli Wang	
Electrical Resistivity Behavior of Loess Specimens during Unconfined Compression Test	40
Zhibin Liu, Songyu Liu, Xin Ma, and Chuanbin Wu	
Some Recent Developments in the Determination of Atterberg Limits	48
Paul J. Vardanega and Stuart K. Haigh	
Evaluating the Performance of a Chilled Mirror Device for Soil Total Suction Measurements	56
Sruthi Mantri and Rifat Bulut	
Internal Sand Deformation around a Tunnel Boring Machine	65
Jinyuan Liu and Jizhu Sun	
Experimental Study on Improving the Frost Heave of Graded Gravel on Passenger-Dedicated Railway Line	73
Zhi-Hong Nie, Yuan Liu, and Xiang Wang	
Modeling and Simulation for Complex Faults of Large-Scale Underground Caverns Based on FLAC^{3D}	81
Shuangying Zuo, Ming Xiao, and Jun Chen	

Back Analysis of Hydraulic Properties for a Landslide in the Three Gorges Area	89
Kun Song, Echuan Yan, Guodong Zhang, and Qinglin Yi	
Experimental Study on the Disintegration Behavior of Granite Residual Soil	98
Xiaowen Zhou, Pan Liu, and Zexin Lan	
Change of Cyclic and Postcyclic Shear Behavior of Low-Plasticity Silt Due to the Addition of Clay	105
Shuying Wang and Jinqiang Zhou	
Prediction of Unsaturated Soil Diffusivity Coefficient from SWCC and Saturated Permeability Tests	113
Yi Tian and Rifat Bulut	
Piecewise-Linear Modeling of Combined Vacuum and Surcharge Preloading at the Second Bangkok International Airport	122
Keith Doyle and Tong Qiu	
Experimental Study on the Unconfined Compressive Strength of Completely Weathered Granite Improved Soil	131
Wen Yi, Zi-Xin Xie, and Yong-He Wang	
Research on the Change Rules of Longitudinal Wave Velocity and the Rebound Value of Sandstone under Water-Rock Interaction	137
Huafeng Deng, Qian Luo, Yayun Hu, and Meiling Zhou	

Discrete Element Method Simulation of Granular Column Collapse

Elnaz Kermani^{1,2}, S.M.ASCE, Tianbin Li³, and Tong Qiu^{2,4}, M.ASCE, P.E.

¹Graduate Research Assistant, Department of Civil and Environmental Engineering, The Pennsylvania State University, University Park, PA 16802, USA; Email: elnaz@psu.edu

²Affiliated Researcher, State Key Laboratory of Geohazard Prevention and Geoenvironment Protection, Chengdu University of Technology, Chengdu, 610059, P.R.China

³Professor, State Key Laboratory of Geohazard Prevention and Geoenvironment Protection, Chengdu University of Technology, Chengdu, 610059, P.R.China; ltb@cdut.edu.cn

⁴Assistant Professor, Department of Civil and Environmental Engineering, The Pennsylvania State University, University Park, PA 16802, USA; Email: tqiu@enr.psu.edu (corresponding author)

ABSTRACT: Understanding of various natural phenomena and industrial processes such as landslides and bulk material handling requires research on the flow of granular materials. In this study, a 3-D numerical investigation of axisymmetric collapse of granular columns has been conducted using a commercial and research discrete element method (DEM) code. The simulated granular columns have an initial radius and height of 5.68 mm and 5.71 mm, respectively, rendering an initial aspect ratio (height/radius) of approximately 1.0. The columns consist of uniform spherical quartz particles with a diameter of 0.32 mm. The nonlinear particle-particle contact behavior and rotational resistance are indirectly accounted for in the DEM model. Comparison between the simulated final deposit morphology (e.g., final height and runout distance) with experimental results that are readily available in literature reveals the importance of rotational resistance in realistic simulations of granular column collapse.

INTRODUCTION

Better understanding of various important phenomena in nature (e.g., landslides) and in industry (e.g., bulk material handling) requires studying the flow of granular materials. Axisymmetric collapse of granular columns has been investigated in several experimental studies (e.g., Lube et al., 2004; Lajeunesse et al., 2004) using granular columns made up of different materials (e.g., sand and glass beads) with different aspect ratios $a = h_i/r_i$, where h_i and r_i are the initial height and radius of the granular column, respectively. The scope of these studies was to correlate the final

height and runout distance of the final deposit to different factors such as properties of materials and experimental setup (e.g., aspect ratio and roughness of underlying surface).

It was observed that the final deposit morphology is dominated by the initial aspect ratio a . For $0 < a < 0.74$, a circular undisturbed region remains at the initial height; for $a > 0.74$, the final deposit takes a cone shape, which according to Lajeunesse et al. (2004) has a lower height than the initial height, while based on Lube et al. (2004) the cone preserves its original height up to $a = 1.7$ and then starts to decrease. The final runout distance based on Lube et al. (2004) depends only on the aspect ratio and initial radius and is independent of subsurface roughness. It was also noted that the inter-particle friction affects the flow pattern only in the last instant when the flow comes to an abrupt stop. On the other hand, Lajeunesse et al. (2004) stated that the grain properties and underlying surface properties play a significant role in the final deposit shape in high aspect ratios.

Several numerical simulations have been also conducted to reproduce the results of aforementioned experimental studies in both continuum and discrete element frameworks and to improve the understanding of the macro- and micro-scale behaviors of the granular flow. Chen and Qiu (2012) successfully used Smoothed Particle Hydrodynamics (SPH) method (Lucy 1977; Gingold and Monaghan, 1977) to simulate the global behavior of the flow within the continuum framework. Discrete element method (DEM, Cundall and Strack, 1979) was also utilized by many researchers (e.g., Staron and Hinch 2005 and 2007; Zenit, 2005; Cleary and Frank, 2006) to capture the discrete and micromechanical behaviors of the granular collapse.

This paper presents the results of a 3-D numerical simulation of the axisymmetric collapse of granular columns using a commercial and research DEM code, *PFC3D 4.0* (Particle Flow Code in three dimensions, Itasca 2008). The main focus is a parametric study to investigate the effect of particle rotational resistance on the final deposit morphology for a column with $a = 1.0$. In the following sections, a brief summary of the DEM model will first be presented, followed by the results of the parametric study.

DEM MODEL

Discrete Element Method (DEM) was originally proposed by Cundall and Strack (1979). In this Lagrangian method, the motion of individual particles is calculated by numerical integration of Newton's equations of motion. Contact forces are calculated based on particle overlaps using contact properties (e.g., stiffness, friction, and damping) (Itasca 2008; O'Sullivan, 2011). This section presents the DEM model used in this study.

Numerical Sample Preparation

The initial model was created by pouring 20,340 balls with a diameter of 0.32 mm into a cylindrical wall of radius r_i , and allowing the balls to settle under gravity. The column was then trimmed to achieve an initial model with radius and height of 5.68 mm and 5.71 mm, respectively, forming a specimen with $a \approx 1$. The porosity of the specimen was approximately 0.40. Fig. 1 presents the initial setup of a granular column. The cylindrical wall was then lifted with a constant velocity of 0.02 m/s to

match the experimental conditions in Lube et al. (2004) and Lajeunesse et al. (2004) and then the packing was allowed to collapse over the bottom wall.

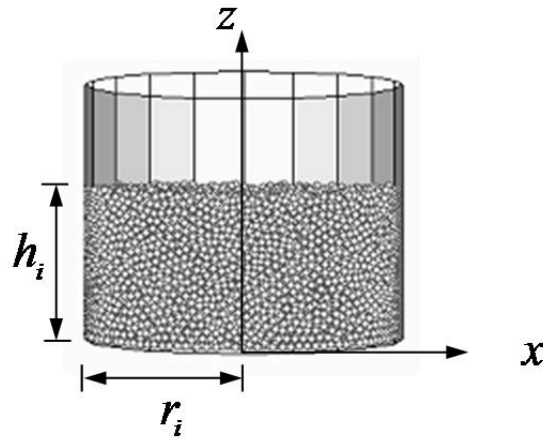


FIG. 1. Initial setup of a granular column.

Material Properties

Particles properties such as particle diameter (D), density (ρ_s), shear modulus (G), Poisson's ratio (ν), friction coefficient (μ), restitution parameters (e), and viscous damping coefficient (ξ) are summarized in Table 1. Value of e was assumed to be 0.75 (Zenit 2005) and was verified by several simple experiments conducted in this study by dropping a glass bead over various glass surfaces. The value of ξ at contact is then calculated as (Itasca 2008; O'Sullivan 2011)

$$\xi = \frac{-\ln(e)}{\sqrt{\ln^2(e) + \pi^2}} \quad (1)$$

Table 1. Material Properties used in DEM Simulation

D	ρ_s	G	ν	μ	e	ξ
0.32 mm	2650 Kg/cm ³	2.9E10 N/m ²	0.3	0.445	0.75	0.0912

Contact Stiffness

In *PFC3D* linear contact model and non-linear Hertz-Mindlin contact model can be considered to evaluate the inter-particle forces. The former is simple and computationally efficient, and is based on constant normal and tangential stiffness. The latter is widely accepted in geotechnical engineering and is an approximation of the theory of Mindlin and Deresiewicz (1953), which assumes the contact stiffness is dependent on the elastic properties of particles, overlap, and normal contact force. Due to the required computational effort, in this study a hybrid approach similar to the work of Teufelsbauer et al. (2009) was utilized, where the linear model is used for the

main simulations but the contact stiffness values are calibrated based on the Hertz–Mindlin model.

The value of secant normal (k_n) and secant shear contact stiffness (k_s) between two identical spherical particles can be evaluated by (Mindlin and Deresiewicz 1953; and Itasca 2008)

$$k_n = \frac{2G \times \sqrt{2R}}{3 \times (1 - \nu)} u^{\frac{1}{2}} \quad (2)$$

$$k_s = \frac{4[3G^2(1 - \nu)R]^{\frac{1}{3}}}{3(2 - \nu)} F_n^{\frac{1}{3}} \quad (3)$$

where R is radius of the particles; u is particle-particle overlap; and F_n is the normal contact force and can be calculated as

$$F_n = \frac{2G \times \sqrt{2R}}{3 \times (1 - \nu)} u^{\frac{3}{2}} \quad (4)$$

According to Eqs. (2) through (4), in order to calculate k_n and k_s , value of u is required. This value varies within the model during the collapse. However, for computational efficiency, one average value for u is selected during the initial, intermediate and final stages of collapse based on the Hertz-Mindlin model. The obtained equivalent k_n and k_s values were later used in the linear model for the parametric study. Therefore, the proposed hybrid approach indirectly accounts for the nonlinear contact behavior and is computationally efficient. The particles in contact are acting in series; hence the ball stiffness should be taken as twice the ball-ball contact stiffness (Itasca 2008). The wall stiffness can be similarly determined based on the average ball-wall overlap, ball-wall contact stiffness, and ball stiffness. The obtained average values of u , k_n and k_s for granular column with aspect ratios of 1.0 are presented in Table 2.

Table 2. Equivalent Normal and Shear Stiffness

For balls			For walls		
u (m)	k_n (N/m)	k_s (N/m)	u (m)	k_n (N/m)	k_s (N/m)
3.07E-10	17000	14000	2.70E-10	15000	12500

Rotational Resistance

In order to consider the effect of particle shape and hysteretic behavior at contacts (e.g., micro-sliding, visco-elasticity, and plasticity), rotational resistance should be applied in DEM simulations (Wensrich and Katterfeld, 2012). This factor can be

considered by either implementing resisting moments on contacting particles (e.g., Zhou et al., 1999; Wensrich and Katterfeld, 2012; Liu et al., 2012) or directly reducing the angular velocity of particles (e.g., Teufelsbauer et al., 2009). In this study, the method proposed by Teufelsbauer et al. (2009) was simplified and used to reduce the angular velocity (ω) of a particle by a constant factor. For the simulations conducted by Teufelsbauer et al. (2009), this factor was approximately 0.99. A parametric study is conducted to investigate the effect of the rotational resistance on the final height and runout distance of the granular column. Three values of the angular-velocity reduction factor: 0.99, 0.95 and 0.90 are considered, which are intended to include varying degrees of rotational resistance arising from the effect of particle shape, particle size distribution, and different test conditions between the experiments of Lube et al. (2004), Lajeunesse et al. (2004), and Teufelsbauer et al. (2009).

RESULTS AND DISCUSSIONS

During these simulations, the deposit height was continuously monitored. The final profile was achieved when the deposit height became relatively constant as shown in Fig. 2. Fig. 3 presents the final deposit profile for a typical simulation, showing the final height h_∞ and final run out distance r_∞ .

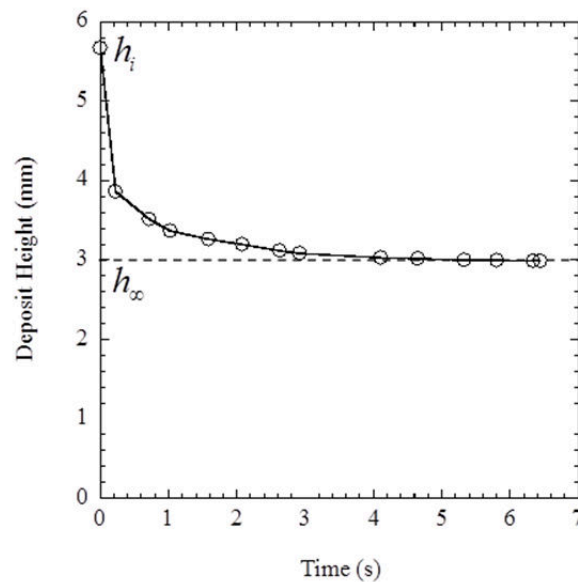


FIG. 2. Deposit height versus time.

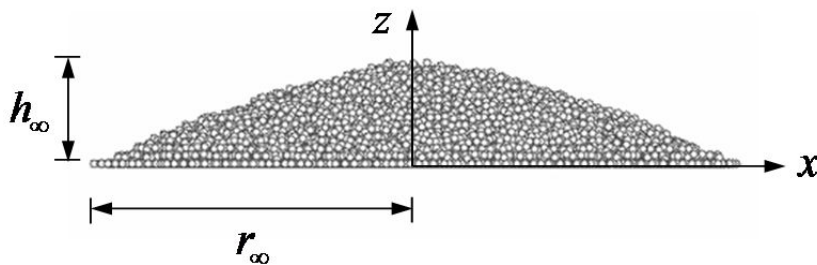


FIG. 3. Final deposit profile.